Tribological Properties of WC/12Co Cermet - Fe-Based Metallic Glass Spray Coating†

TERAJIMA Takeshi*, TAKEUCHI Fumiya, NAKATA Kazuhiro***, ADACHI Shinichiro****, NAKASHIMA Koji***** and IGARASHI Takanori*****

Abstract

A composite coating containing WC/12Co cermet and $Fe_{43}Cr_{16}Mo_{16}C_{15}B_{10}$ metallic glass was successfully deposited onto type 304 stainless steel by high-velocity oxygen fuel (HVOF) spraying, and the microstructure and tribological properties were investigated. The microstructure of the coating was characterized by scanning electron microscopy/electron probe micro-analysis (SEM/EPMA) and X-ray diffractometry (XRD). The hardness and tribological properties of the coating were tested with a Vickers hardness tester and reciprocating wear tester, respectively. The composite coating, in which flattened WC/12Co was embedded in amorphous $Fe_{43}Cr_{16}Mo_{16}C_{15}B_{10}$ layers, exhibited high hardness, good wear resistance and a low friction coefficient compared to the monolithic coating. The addition of 8% WC/12Co to the $Fe_{43}Cr_{16}Mo_{16}C_{15}B_{10}$ matrix increased the cross-sectional hardness from 660 to 870 HV and reduced the friction coefficient from 0.65 to 0.5. WC/12Co reinforcement plays an important role in improving the tribological properties of the $Fe_{43}Cr_{16}Mo_{16}C_{15}B_{10}$ coating.

KEY WORDS: (Metallic glass), (Cermet), (High-velocity oxygen fuel spraying), (Tribological property), (Spray coating)

1. Introduction

Fe-based metallic glass has unique properties in terms of mechanical strength, hardness and corrosion resistance[1-3]. These excellent characteristics originate from atomic disorder and thus are not found in crystalline metals. Therefore, Fe-based metallic glass is a suitable coating material for corrosion and wear protection.

Thermal plasma spraying is a convenient method for applying a thick amorphous coating[4-6]. During the plasma spray process, the starting powder is melted in a plasma torch and then quenched on a substrate. The critical cooling rate required to form an amorphous structure is approximately 10 K/s in the case of Fe-based metallic glass[7]. Thus, it is difficult to produce homogeneous amorphous coating by the liquid-quench process. Furthermore, the plasma spray coating does not afford sufficient protection against corrosion and wear due to defects such as lamellar structures and pores which are unique in plasma spray coating.

Recently, interest has grown in the use of high-velocity oxygen fuel spraying (HVOF) for the application of surface protective coatings[8, 9]. A key feature of HVOF is that a high-density coating can be obtained since the starting powder collides with the substrate at a supersonic velocity and is severely deformed. Another key feature is that the process temperature is close to the range of the glass transition temperatures of metallic glasses. Around the glass transition temperature, metallic glass transforms into a supercooled state and shows viscous fluidity in spite of temperatures far below its liquidus temperature. Therefore, high-quality metallic glass coatings can be achieved using HVOF spraying.

Recently, studies of Fe-based metallic glass coatings that were applied by the HVOF process have appeared in the literature[10-12]. These reports demonstrated that the Fe-based metallic glass coating remains amorphous after spraying and shows good adhesion to the substrate. However, it was found in the preliminary study that the $Fe_{43}Cr_{16}Mo_{16}C_{15}B_{10}$ metallic glass coating exhibited a very low friction coefficient in a lubricating oil environment but a high friction coefficient in a dry environment. Therefore, the monolithic $Fe_{43}Cr_{16}Mo_{16}C_{15}B_{10}$ coating was relatively poor at protecting against wear. One way of improving the tribological properties of $Fe_{43}Cr_{16}Mo_{16}C_{15}B_{10}$ coating is to modify its contact surface. The tribological properties

† Received on July 10, 2009
* Specially Appointed Assistant Professor
** Graduate Student
*** Professor
**** Technology Research Institute of Osaka Prefecture
***** Topy Industrial CO., LTD.
Transactions of JWRI is published by Joining and Welding Research Institute, Osaka University, Ibaraki, Osaka 567-0047, Japan

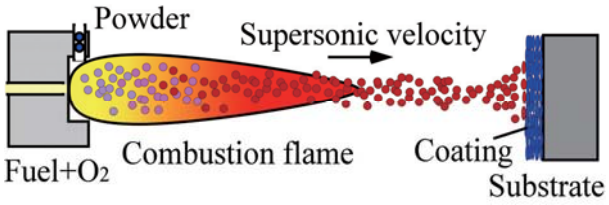

Fig.1 Schematic illustration of High Velocity Oxygen Fuel Spraying (HVOF).

can be considerably influenced by adding second-phase reinforcement such as hard WC/12Co metal. In this study, the production of a WC/12Co–$Fe_{43}Cr_{16}Mo_{16}C_{15}B_{10}$ composite coating via the HVOF process was demonstrated, and the microstructure and tribological properties were investigated.

2. Experimental

$Fe_{43}Cr_{16}Mo_{16}C_{15}B_{10}$ (atom %) metallic glass powder was prepared by gas atomization. The particle size was 10-25 μm in diameter. The glass transition temperature T_g and crystallization temperature T_x as measured by differential scanning calorimetry (DSC) at a heating rate of 20 K/min were 875 K and 941 K, respectively. The reinforcement used in this study was commercial WC/12Co (Co: 12 wt %) cermet powder having particle sizes of 5-25 μm in diameter. $Fe_{43}Cr_{16}Mo_{16}C_{15}B_{10}$ and WC/12Co powders were homogeneously mixed before spraying. A commercial HVOF spraying system (JP-5000, Praxair Technology Inc., USA), which generates a supersonic flame by combusting a mixture of kerosene and oxygen, was used to spray these powders onto a stainless steel substrate as illustrated in **Fig. 1**. The flow rates of kerosene and oxygen were 0.3 L/min and 850 L/min, respectively. The dimensions of the type 304 stainless steel substrate were 50×50×5 mm, and its surface was blasted by steel grit to improve adhesion. The composite coating was deposited with a thickness of 250-300 μm on the substrate by 16 transverses of the flame gun.

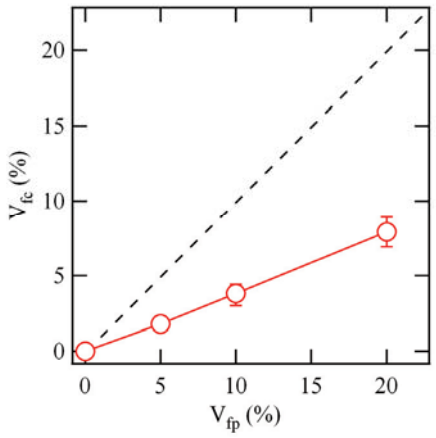

Fig.2 The relation of the volume fraction of WC/12Co in the starting powder, V_{fp}, to that in the coating, V_{fc}. Dot line is a supplement plot (V_{fc}=V_{fp}).

The microstructure of the cross section of the coating was observed by scanning electron microscopy (SEM) and electron probe micro-analysis (EPMA). Volume fraction of the WC/12Co was determined by the total area of WC/12Co on the cross section of the coating. Crystalline phases of the starting powder and the sprayed coatings were identified by X-Ray diffractometry (XRD) using Cu K_α radiation. The apparent Vickers hardness on the cross section and surface of the coating was measured using a micro Vickers hardness tester at a load of 0.98 N. The measurements were repeated at 20 points on the sample and the results were averaged. The wear properties were measured using a reciprocating wear tester by a sliding ϕ4.8 mm Al_2O_3 ball at a load of 1.96 N. A lubricant oil was not used in the wear test. The sliding speed and total sliding time were 20 mm/s and 7200 s, respectively. The abrasion area S of the cross section of the wear track was measured with a stylus surface profiler (Dektak3, Ulvac Co., Ltd.). The specific wear amount W_s was calculated according to the following equation:

$$W_s = \frac{AS}{PL} \qquad (1)$$

where A, P and L are sliding amplitude (5 mm), load (1.96 N) and total sliding distance (144 m), respectively. The friction coefficient was averaged in the range of sliding distance from 72 m to 144 m, in which the value

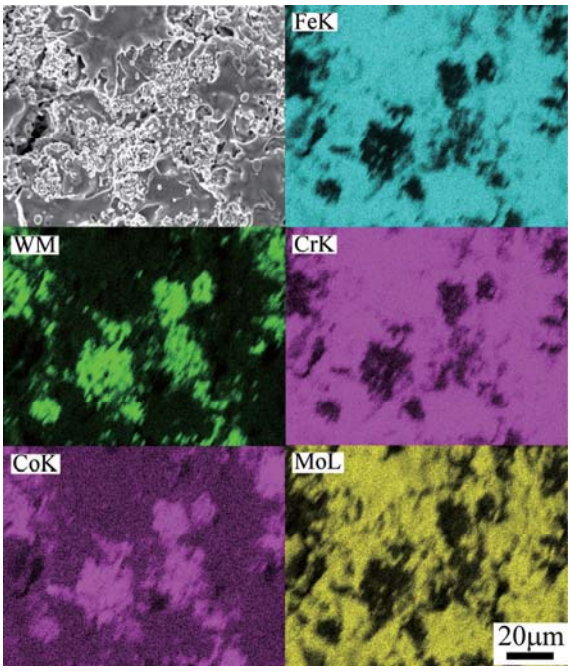

Fig.3 Element maps on the surface of $Fe_{43}Cr_{16}Mo_{16}C_{15}B_{10}$ coating containing 8% WC/12Co.

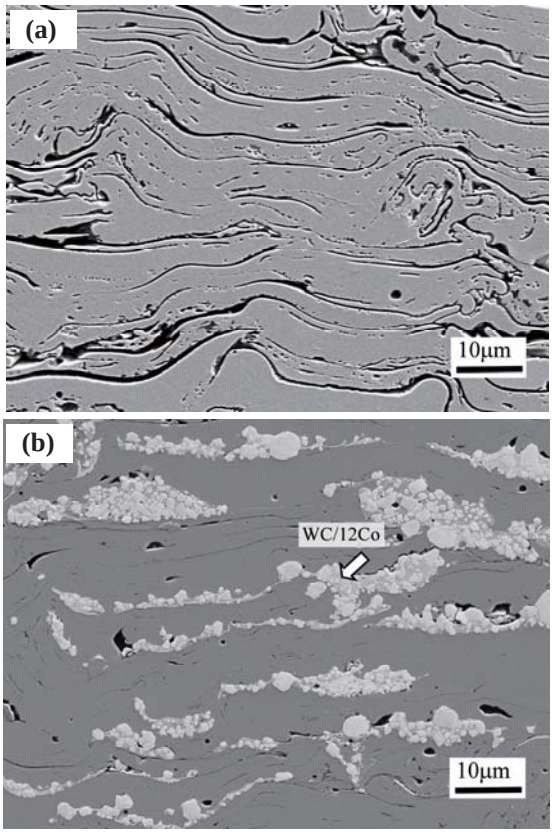

Fig.4 SEM images of the cross section of $Fe_{43}Cr_{16}Mo_{16}C_{15}B_{10}$ coating containing **(a)** 0% and **(b)** 8% WC/12Co.

of the friction coefficient was stable.

3. Results and Discussion

The $Fe_{43}Cr_{16}Mo_{16}C_{15}B_{10}$ powder was successfully prepared by the atomization method. $Fe_{43}Cr_{16}Mo_{16}C_{15}B_{10}$ powder contained mostly spherical particles of ϕ10-25 μm, although some cylindrical particles were also present. WC/12Co powder consisted of spherical particles of ϕ5-25 μm and was porous. The relation of the volume fraction of WC/12Co in the starting powder, V_{fp}, to that in the coating, V_{fc}, is shown in **Fig.2**. By using starting powders containing 0, 5, 10 and 20 vol % WC/12Co, composite coatings containing 0, 2, 4 and 8 % WC/12Co were obtained, respectively. This means that approximately 40% of the WC/12Co in the starting powder was taken in the coating. **Fig.3** shows the element maps on the surface of coating containing 8% WC/12Co. WC/12Co powder, whose distribution was corresponded to the W and Co maps, was flattened to a disk shape with 30-40 μm in diameter. It covered approximately 20 area% of the coating surface. **Fig. 4(a) and (b)** shows the cross-sectional microstructure of the coatings containing 0 and 8% WC/12Co, respectively. The microstructure exhibited the typical layered structure that is unique to spray coating. EPMA analysis confirmed the dark lamellae to be $Fe_{43}Cr_{16}Mo_{16}C_{15}B_{10}$, while the bright

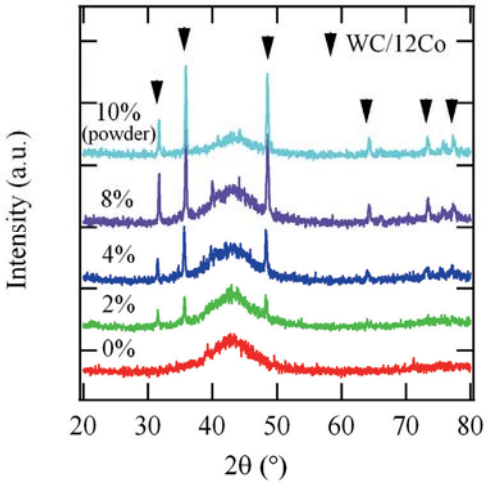

Fig.5 XRD patterns of starting powder and WC/12Co–$Fe_{43}Cr_{16}Mo_{16}C_{15}B_{10}$ composite spray coatings.

lamellae were identified as WC/12Co. The high-velocity impact of the $Fe_{43}Cr_{16}Mo_{16}C_{15}B_{10}$ powder on the substrate in the supercooled state results in severe plastic deformation and rapid solidification. Therefore, the HVOF spray coating layers were closely adhered to each other. The average porosity fraction in the monolithic $Fe_{43}Cr_{16}Mo_{16}C_{15}B_{10}$ coating was 3%. This decreased to 1% in the coating containing 2% WC/12Co since the WC/12Co splat filled the vacancy between $Fe_{43}Cr_{16}Mo_{16}C_{15}B_{10}$ lamellae. In contrast, the porosity increased to 1.6 and 2.6% in the coating containing 4 and 8% WC/12Co, respectively, due to the vacancies that initially existed inside the WC/12Co powder. **Fig. 5** shows XRD patterns of the starting powder containing

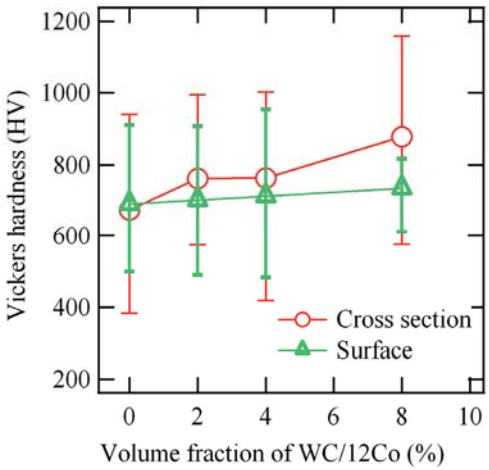

Fig.6 Vickers hardness on the surface and the cross section of WC/12Co–$Fe_{43}Cr_{16}Mo_{16}C_{15}B_{10}$ composite spray coatings.

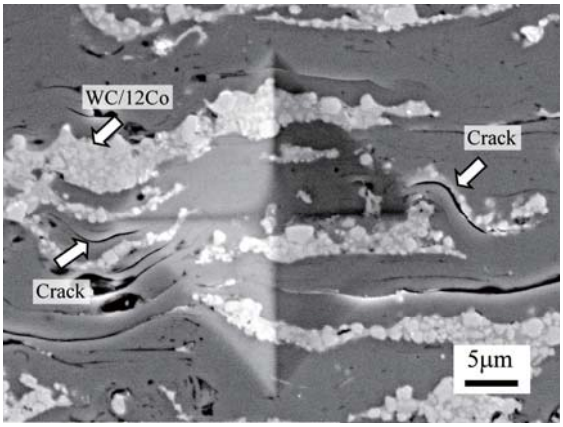

Fig.7 Trace of indentation on the $Fe_{43}Cr_{16}Mo_{16}C_{15}B_{10}$ coating containing 8% WC/12Co.

10% WC/12Co and the sprayed coatings. Diffraction peaks of WC and the halo pattern between 35° and 50° attributed to amorphous $Fe_{43}Cr_{16}Mo_{16}C_{15}B_{10}$ were observed. These indicate that the atomic disorder of the starting powder was maintained in the sprayed coatings, and no significant decomposition, alloying or oxidation occurred during the spraying process.

Fig. 6 shows the micro Vickers hardness of the surface and the cross section of the coating. The cross-sectional hardness of the monolithic $Fe_{43}Cr_{16}Mo_{16}C_{15}B_{10}$ coating was approximately 660 HV. As the volume fraction of WC/12Co increased, the Vickers hardness gradually increased and reached a value of 870 HV at 8% WC/12Co. In contrast, surface hardness was not considerably affected by the WC/12Co fraction. This anisotropy corresponds to the structure of the coating in which flattened WC/12Co is oriented parallel to the coating surface. The trace of the indentation made by the Vickers test is shown in **Fig. 7**. This shows that the indenter contacted not only $Fe_{43}Cr_{16}Mo_{16}C_{15}B_{10}$ layers but also hard WC/12Co layers. WC/12Co reinforcement likely helps to increase hardness. However, the Vickers hardness of the sprayed composite coating was even lower than that of bulk material since the coating often cracked along the interfaces between the lamellae of the $Fe_{43}Cr_{16}Mo_{16}C_{15}B_{10}$ layers from the corner of the indent where the stress produced by indentation was highest.

Fig. 8(a) shows friction coefficients of the coating containing 0, 2, 4 and 8% WC/12Co. During the initial stage of the reciprocating wear test, the friction coefficient was unstable due to highly adhesive micro-contact between the coating and the Al_2O_3 ball. The friction coefficient averaged in the sliding distance from 72 to 144 m and the specific wear amount is shown in **Fig. 8(b)**. It is worth noting that the value of the friction coefficient is not an apparent function of the WC/12Co fraction. However, it did decrease from 0.65 to 0.5, which is close to the value of 0.4 for the monolithic WC/12Co coating as a result of increasing WC/12Co solid lubricant. Furthermore, the presence of 2-8% WC/12Co drastically reduced the specific wear amount from 0.8×10^{-4} to 0.1×10^{-4} mm^3 N^{-1} m^{-1}. It is clear that the WC/12Co–$Fe_{43}Cr_{16}Mo_{16}C_{15}B_{10}$ composite coatings have better tribological properties than the monolithic coating.

Fig. 9(a) and (b) shows SEM images of the wear tracks of the monolithic $Fe_{43}Cr_{16}Mo_{16}C_{15}B_{10}$ coating and the composite coating containing 8% WC/12Co, respectively. As shown in **Fig. 9(b)**, the WC/12Co was uniformly distributed and strongly bonded to the $Fe_{43}Cr_{16}Mo_{16}C_{15}B_{10}$ matrix and the wear tracks are clearly visible parallel to the sliding direction. This track seems to be formed by scratching by the WC debris produced during the wear test since it is not clearly visible for the monolithic $Fe_{43}Cr_{16}Mo_{16}C_{15}B_{10}$ coating as shown in **Fig. 9(a)**. WC/12Co reinforcement plays an important role in the reduction of the friction coefficient

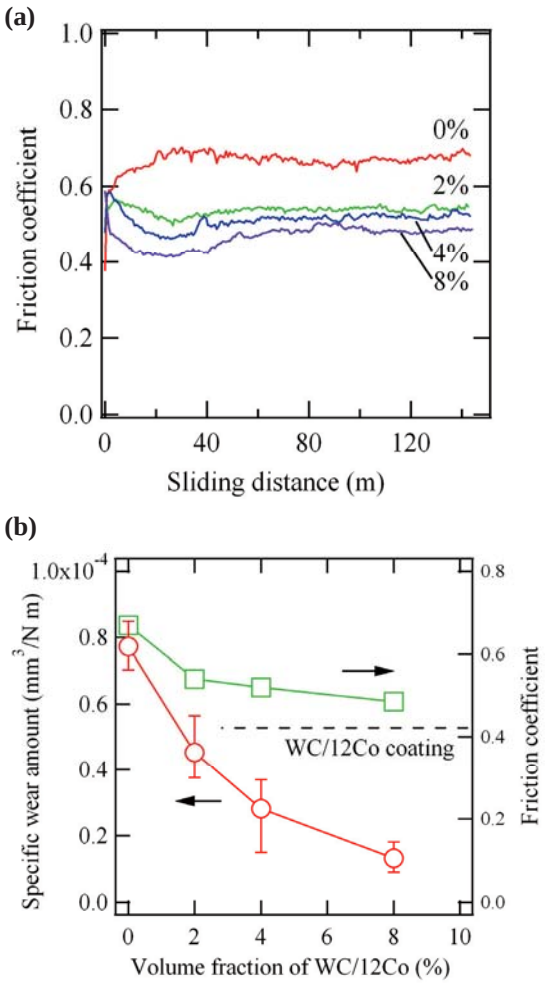

Fig.8(a) Friction coefficients of the WC/12Co–$Fe_{43}Cr_{16}Mo_{16}C_{15}B_{10}$ composite spray coatings. **(b)**Specific wear amount and friction coefficients averaged in the sliding distance from 72 to 144m.

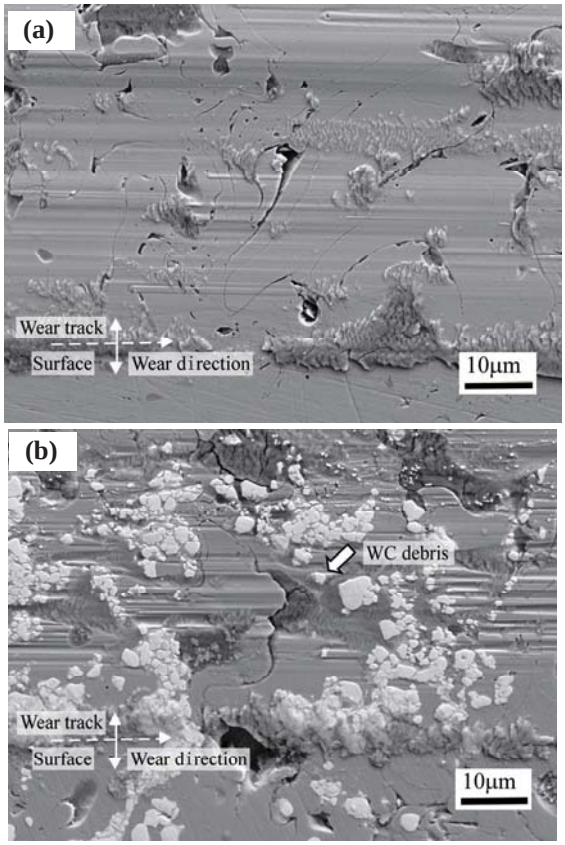

Fig.9 SEM images of wear tracks of (a) monolithic $Fe_{43}Cr_{16}Mo_{16}C_{15}B_{10}$ coating and (b) $Fe_{43}Cr_{16}Mo_{16}C_{15}B_{10}$ coating containing 8% WC/12Co.

and prevention of wear abrasion caused by the Al_2O_3 ball.

4. Conclusions

WC/12Co–$Fe_{43}Cr_{16}Mo_{16}C_{15}B_{10}$ metallic glass composite coating deposited by an HVOF spraying process was demonstrated, and its tribological properties were investigated. The sprayed coatings were successfully coated onto stainless steal without crystallization, decomposition, alloying or oxidation. As the fraction of WC/12Co increased from 0 to 8%, the cross-sectional hardness of the coating increased from 660 to 870 HV; however, surface hardness was little changed. Furthermore, addition of 8% WC/12Co improved the specific wear amount and decreased the friction coefficient from 0.65 to 0.5. It was found that WC/12Co plays important role in improving the tribological properties of the $Fe_{43}Cr_{16}Mo_{16}C_{15}B_{10}$ coating.

References

1) S. J. Pang, T. Zhang, K. Asami and A. Inoue, Acta. Mater., 50(2002)489-497.
2) M. Iqbal, J. I. Akhter, H. F. Zhang and Z. Q. Hu, J. Non-Cryst. Solids, 354 (2008) 3284-3290.
3) A. Inoue, Acta Mater., 48 (2000) 279-306.
4) A. Kobayashi, S. Yano, H. Kimura and A. Inoue, Surf. Coat. Technol., 202 (2001) 2513-2518.
5) K. Kishitake, H. Era and F. Otsubo, J. Therm. Spray Techno., 5 (1996) 476-482.
6) S. Kumar, J. Kim, H. Kim and C. Lee, J. alloys Comp., 475 (2009) L9-L12.
7) J. Shen, Q. Chen, J. Sun H. Fan and G. Wang, Appl. Phys. Lett., 86 (2005) 151907.
8) J. Koutsky, J. Mater. Proc. Technol., 557-560 (2004) 557-560.
9) H. J. Kim, K. M. Lim, G. G. Seong and C. G. Park, J. Mater. Sci., 36 (2001) 49-54.
10) Y. Wu, P. Lin, G. Xie, J. Hu and M. Cao, Mater. Sci. Eng. A, 430 (2006) 34-39.
11) H. Kim, K. Nakata, T. Tsumura, M. Sugiyama, T. Igarashi, M. Fukumoto, H. Kimura and A. Inoue, Mater. Sci. Forum. 580 (2008) 467-470.
12) K. Chokethawai, D.G. McCartney and P.H. Shipway, J. Alloys Comp., 480 (2009) 351-359